Numerical modeling of evanescent-wave atom optics

C. M. Savage,* D. Gordon, and T. C. Ralph

Department of Physics and Theoretical Physics, The Australian National University, Australian Capital Territory 0200, Australia

(Received 21 April 1995)

We numerically solve the time-dependent Schrödinger equation for a two-level atom interacting with an evanescent light field. The atom may be reflected or diffracted. Using the experimental parameter values we quantitatively model the evanescent field dopplerons (velocity-tuned resonances) observed by Stenlake et al. [Phys. Rev. A **49**, 16 (1994)]. Besides successfully modeling the experiment, our approach provides complementary insights to the usual solution of the time-independent Schrödinger equation. We neglect spontaneous emission.

PACS number(s): 42.50.Vk, 32.80.Pj, 03.75.Be

I. INTRODUCTION

Evanescent light fields have been used to reflect [1–8] and diffract [9] beams of atoms. The theory of these processes is well developed [10–13]. In this paper we quantitatively model the experimental observations of evanescent field dopplerons by Stenlake et al. [8]. Quantitative agreement is achieved without any free parameters.

We compute the dynamics of atomic wave functions undergoing reflection and diffraction by evanescent light. This approach allows the dynamics of the interaction to be studied and hence provides complementary insights to those derived from solutions of the time-independent Schrödinger equation [12,13].

We have numerically solved the time-dependent Schrödinger equation for a two-level atom moving in the evanescent field produced by total internal reflection of two laser beams. Throughout the interaction the wave functions are available in either the coordinate or momentum representations. Previous numerical work has computed atomic transmission and reflection coefficients [14]. The work closest in spirit to ours is that of Janicke and Wilkens [15], who considered magneto-optical configurations. However, they did not attempt quantitative comparisons with specific experiments.

We have successfully modeled the experimental observations of dopplerons (velocity-tuned resonances) [16] in the evanescent-wave reflection of sodium atoms by Stenlake et al. [8]. In particular we have determined the central frequencies and widths of the dopplerons, which are dependent on the transition light shifts. Agreement with experiment is found using parameters that are within the experimental uncertainties. We are able to explain the difficulty of experimentally observing higher order dopplerons by their relatively small depth and width. Our model is also consistent with the experiment in not showing diffraction for fast atom beams. Nevertheless the important limitations of our model are its neglect of spontaneous emission and of the spatial profile of the laser beams.

II. THE MODEL AND ITS NUMERICAL SOLUTION

We focus on the diffraction of an atom by the evanescent light field associated with two laser beams totally internally reflected from a glass-vacuum interface. The direction perpendicular to the glass is y and the direction parallel to the glass x. The origin of the y coordinate is at the interface and the positive direction is into the vacuum. We assume that the atom is initially propagating towards the interface in the x-y plane with a positive x component of velocity; see Fig. 1.

The atom has two levels, a ground level $|-\rangle$ and an excited level $|+\rangle$, separated by energy $\hbar\omega_a$. The Hamiltonian for the system comprises the kinetic energy of the atom with center of mass momentum $\hat{\mathbf{p}}$, the internal energy of the atom, and the electric dipole interaction between these levels and the electric field $E(t,\hat{\mathbf{r}})$,

$$\hat{H} = \hat{\mathbf{p}}^2/2m + \hbar\omega_a\hat{\sigma}_+\hat{\sigma}_- + \hbar g(\hat{\sigma}_+ + \hat{\sigma}_-)E(t,\hat{\mathbf{r}}). \quad (1)$$

The mass of the atom is m, $\hat{\sigma}_+$ and $\hat{\sigma}_-$ are the raising and lowering operators for the transition, $\hbar g$ is the dipole moment of the transition, t is time, and $\hat{\mathbf{r}}$ is the position operator for the atom's center of mass. We denote operators by carets.

The experiment we model reflected sodium atoms from a grating made by two counterpropagating laser beams. The evanescent electric field is modeled by

$$E(t,\hat{\mathbf{r}}) = \exp(-q\hat{y})\{(E_1\exp[-i(\omega_1 t - Q\hat{x})] + \text{H.c.})$$
$$+ (E_2\exp[-i(\omega_2 t + Q\hat{x})] + \text{H.c.})\}, \quad (2)$$

where H.c. means the Hermitian conjugate of the preceding terms. This form assumes that the fields are uniform in the x direction and hence does not include the Gaussian spot shape
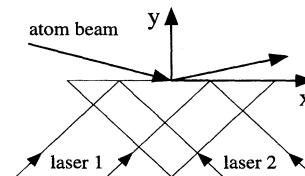

FIG. 1. Geometry of the lasers and atomic beam in the evanescent field reflection experiment.

* Electronic address: Craig.Savage@anu.edu.au

of the laser beams. Quantities associated with the beams co-propagating and counterpropagating with respect to the atoms are denoted by subscripts 1 and 2, respectively. The field amplitudes are E_i and the laboratory frame angular frequencies are ω_i. The evanescent-wave wave number is $Q = n \sin(\theta) k$, where $n = 1.46$ is the refractive index of the quartz block, $\theta = \pi/4$ rad is the angle of incidence of the totally internally reflected laser beams, and $k = 1.066 \times 10^7$ m^{-1} is their vacuum wave number [8]. The inverse evanescent field decay length is $q = k \sqrt{[n \sin(\theta)]^2 - 1}$. We have assumed that the wave numbers of the two fields are sufficiently close that they can be approximated by $k = k_1 \approx k_2$. This greatly reduces the computational problem because the x component of the atomic momentum only changes by $\pm \hbar Q$ for each absorbed or emitted photon. We have also made the rotating-wave approximation by ignoring energy nonconserving terms in the dipole interaction. This approximation will have a negligible effect on time scales that are much longer than the optical period.

With these approximations, and in the interaction picture with the atomic dipole rotating at frequency $\bar{\omega} = (\omega_1 + \omega_2)/2$, the Hamiltonian becomes

$$\hat{H}' = \hat{\mathbf{p}}^2/2m + \hbar(\omega_a - \bar{\omega})\hat{\sigma}_+ \hat{\sigma}_- + \hbar g \exp(-q\hat{y})$$
$$\times \{\hat{\sigma}_+ (E_1 \exp[-i(\Delta_d t - Q\hat{x})]$$
$$+ E_2 \exp[i(\Delta_d t - Q\hat{x})]) + \text{H.c.}\}, \tag{3}$$

where we have introduced the laboratory frame detuning between the two fields, $\Delta_d = (\omega_1 - \omega_2)/2$.

We assume that the atoms are initially in their ground level $|-\rangle$ and in an eigenstate $|k_{0x}\rangle$ of the x component of their momentum with eigenvalue $\hbar k_{0x}$. Then because the photon momentum of the copropagating field is $\hbar Q$ and that of the counterpropagating field $-\hbar Q$, the x component of the momentum of the atoms is restricted to the eigenvalues $\hbar(k_{0x} + nQ)$, with n any integer. When the atom is in its excited level $|+\rangle$, n is odd, and when the atom is in its ground level $|-\rangle$, n is even. We calculate the wave functions $\psi_n(y,t)$ occurring in the following ansatz for the atom's quantum state $|x,y,t\rangle$:

$$|x,y,t\rangle = \exp(-i\hbar k_{0x}^2 t/2m)$$
$$\times \left\{ \sum_{n,\text{even}} \psi_n |-\rangle |k_{0x} + nQ\rangle \exp(-in\Delta_d t) \right.$$
$$\left. + \sum_{n,\text{odd}} \psi_n |+\rangle |k_{0x} + nQ\rangle \exp(-in\Delta_d t) \right\}. \tag{4}$$

We substitute this ansatz into the Schrödinger equation associated with the Hamiltonian Eq. (3) to find the following system of equations for the wave functions:

$$i\partial_t \psi_n = \left\{ \frac{\hat{p}_y^2}{2m\hbar} + S_n \right\} \psi_n + g \exp(-qy)(E_1^* \psi_{n+1}$$
$$+ E_2^* \psi_{n-1}) \quad , \quad n \text{ even}, \tag{5a}$$

$$i\partial_t \psi_n = \left\{ \frac{\hat{p}_y^2}{2m\hbar} + S_n + \omega_a - \bar{\omega} \right\} \psi_n + g \exp(-qy)(E_1 \psi_{n-1}$$
$$+ E_2 \psi_{n+1}) \quad , \quad n \text{ odd}, \tag{5b}$$

$$S_n \equiv \frac{\hbar}{2m}(2k_{0x}nQ + n^2 Q^2) - n\Delta_d. \tag{6}$$

The bracketed terms in S_n describe the Doppler shift and recoil effects. The last term is associated with the energy difference between the field and ground level atom energies.

Equations (5) are multicomponent Schrödinger equations in time and one spatial dimension. The spatial dimension is y, perpendicular to the glass, and the components correspond to x momentum eigenstates, parallel to the glass. Equations (5) may be written in vector form,

$$i\partial_t \mathbf{\Psi} = \left\{ \frac{\hat{p}_y^2}{2m\hbar} + \mathbf{V}(y) \right\} \mathbf{\Psi}, \tag{7}$$

where $\mathbf{\Psi} = \{ \ldots \psi_{-1}, \psi_0, \psi_1, \ldots \}$, and the matrix $\mathbf{V}(y)$ is the discrete part of the Hamiltonian. Separation of the Hamiltonian into kinetic and nonkinetic energy parts is the basis of our numerical method, the "split operator" method, described in detail in Refs. [18,19]. Briefly, it approximates the unitary evolution operator $\hat{\mathbf{U}}$, such that

$$\mathbf{\Psi}(t + \Delta t) = \hat{\mathbf{U}} \mathbf{\Psi}(t) \tag{8}$$

by the following form that gives an error of order $(\Delta t)^3$,

$$\hat{\mathbf{U}} \approx \exp\left(-i\frac{\Delta t}{2}\frac{\hat{p}_y^2}{2m\hbar}\right) \exp(-i\Delta t \mathbf{V}) \exp\left(-i\frac{\Delta t}{2}\frac{\hat{p}_y^2}{2m\hbar}\right). \tag{9}$$

A computational advantage of the method is that the kinetic and nonkinetic energy parts of the evolution reduce to multiplications of the wave functions in their momentum and coordinate representations, respectively. The transformation between representations is efficiently performed by the fast Fourier transform.

One of the specific difficulties of modeling the interaction of atoms with evanescent waves is the treatment of atoms that are not reflected. Such atoms interact with the glass surface and are adsorbed or scattered [17]. This is a dissipative interaction and hence cannot be modeled by a unitary Schrödinger equation. One solution is to introduce a fictitious complex potential and hence solve a nonunitary Schrödinger equation. However, care must be taken to avoid spurious reflections from the complex potential. We model nonreflected atoms by allowing them to propagate into the region $y < 0$. In our model atoms in this region obey the Schrödinger equations (5), but their only physical significance is to represent nonreflected atoms. In this region the model has constant electric fields, which are continuous with the evanescent field at the glass-vacuum interface. The careful treatment of nonreflected atoms is important for the accurate modeling of dopplerons, which we describe in the next section.

III. DOPPLERONS

In this section we compare the results of our model with the experimental observations of doppleron resonances by Stenlake *et al.* [8] and find quantitative agreement. Evidence for dopplerons in evanescent waves has also been reported by Feron *et al.* [7].

In the experiment dopplerons occur when multiphoton transitions from the ground level to the excited level come into resonance as the copropagating laser frequency is scanned. In the laboratory frame the resonance condition depends on the longitudinal velocity of the atom v_x, since this determines the Doppler shifts $v_x Q$ of the field frequencies. The atom-field detunings in the laboratory frame are

$$\Delta_1 = \omega_1 - \omega_a \quad , \quad \Delta_2 = \omega_2 - \omega_a . \tag{10}$$

The analysis of dopplerons is particularly simple in the "grating frame," in which the grating formed by the interference of the counterpropagating lasers is stationary [8]. This frame moves through the laboratory frame with velocity

$$v_g = (\Delta_1 - \Delta_2)/(2Q). \tag{11}$$

In this frame the two lasers have the same frequency and hence the same atomic detuning

$$\Delta' = (\Delta_1 + \Delta_2)/2. \tag{12}$$

The Doppler shift of the fields in the grating frame due to the atomic velocity is

$$\Delta_D' = (v_x - v_g)Q. \tag{13}$$

Weak field multiphoton resonant absorption occurs when the atomic detuning is an odd integer multiple of this Doppler shift,

$$\Delta' = n\Delta_D' \quad , \qquad n \in \text{odd integers}. \tag{14}$$

In the strong fields necessary to reflect atoms the atomic transition frequency is light shifted by an amount Δ_L, so that the doppleron resonance condition becomes

$$\Delta' = n\Delta_D' + \Delta_L \quad , \qquad n \in \text{odd integers}. \tag{15}$$

The light shift Δ_L will vary during the interaction as the evanescent field strength varies with distance from the interface. Hence we expect not only a shift but also a broadening of the doppleron resonance. The sign of the light shift depends on the detuning of the light field. For positive detunings, as in our case, the transition frequency is reduced, so $\Delta_L < 0$.

An example of a numerical solution of the Schrödinger equations (5) for the conditions of the experiment of Stenlake *et al.* [8] is shown in Fig. 2. It shows the probability densities $|\psi_n(y,t)|^2$ before and after partial reflection of Na atoms near an $n = +3$ doppleron. The fraction of atoms reflected is approximately 40%. Only the physical region $y \geq 0$ is shown. For this and subsequent figures the initial wave function is an $n = 0$ Gaussian with mean position $\langle y \rangle$
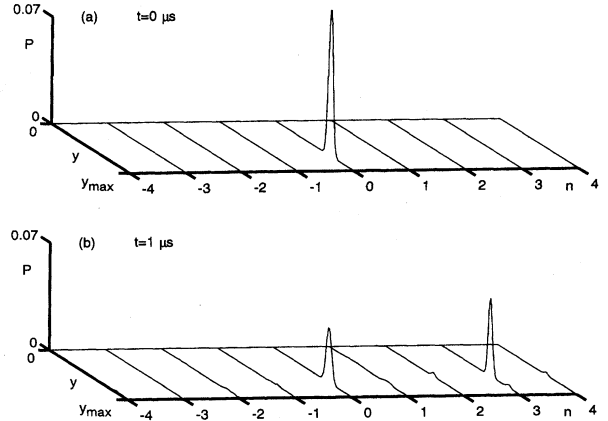

FIG. 2. Coordinate-space probability densities $P = |\psi_n(y,t)|^2$, for $y \geq 0$, for a Na atom undergoing partial reflection near an $n = 3$ doppleron. The quartz surface is at $y = 0$ and $y_{max} = 1.88$ μm. The parameters are given in Table I and correspond to those of the experiment of Stenlake *et al.* [8], with $\Delta_1 = 2\pi \times 2.725$ GHz. (a) $t = 0$, (b) $t = 1$ μs.

and variance $\text{Var}(y)$, as given in Table I. Figure 2 was obtained with a time step of $\Delta t = 0.1$ ns, a y grid of 4096 points with a lattice spacing of 0.92 nm, and using ψ_n for $n \in (-7, -6, \ldots, 6, 7)$, although only $n \in (-4, \ldots, 4)$ are shown. Varying the time step and lattice spacing produced no significant changes in the numerical results.

The outgoing wave function with $n = 3$ is formed from the $n = 0$ wave function *after* reflection has occurred. It corresponds to diffraction at a low angle of about 1.6 mrad. This was not observed in the experiment of Stenlake *et al.* [8] because it represents an excited state with a lifetime of about 16 ns. The 0.5 μs between the reflection of the atom and Fig. 2(b) therefore corresponds to about 30 lifetimes. Hence the

TABLE I. Parameters used to obtain the figures. For Figs. 2 and 3 the velocity and detuning differ slightly from the values given in Ref. [8], since they were adjusted within the experimental uncertainty to improve the fit.

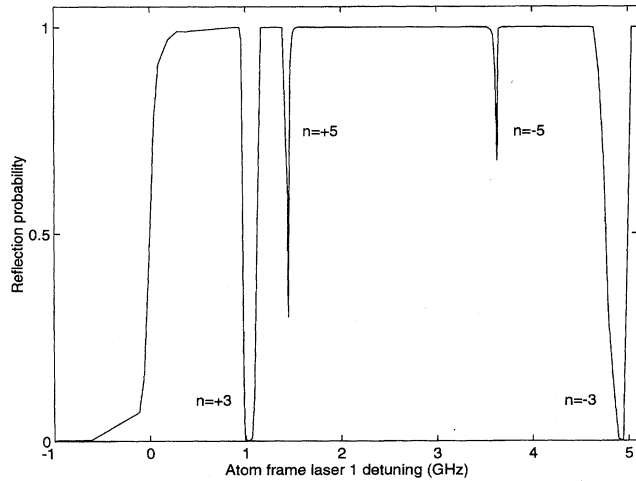| Parameter	Figs. 2,3	Fig. 4	Units
Atom	Na	Ne*	
Atomic velocity	920	20	ms^{-1}
Angle of incidence	2.5	50	mrad
$\langle y \rangle_{t=0}$	1.3	1.1	μm
$\text{Var}(y)_{t=0}$	75	88	nm
Δ_1	See captions	$2\pi \times 68.4$	MHz
Δ_2	$2\pi \times 710$	$2\pi \times 68.4$	MHz
n	1.46	1.56	
k	1.066×10^7	9.82×10^6	m^{-1}
Q	1.10×10^7	1.08×10^7	m^{-1}
q	2.72×10^6	4.57×10^6	m^{-1}
$|gE_1|$	10	0.91	GHz
$|gE_2|$	7.3	0.39	GHz

FIG. 3. Reflection probability versus atom frame detuning of the copropagating laser, $\Delta_1''/2\pi$, Eq. (16). This figure should be compared to Fig. 2 of Stenlake et al. [8]. The parameters are given in Table I. In particular, $\Delta_1 = \Delta_1'' + 2\pi \times 1.61$ GHz. With a dipole moment of $\hbar g = 2 \times 10^{-29}$ cm the intensities of lasers 1 and 2 are, respectively, about 400 W cm^{-2} and half that. The reflection dips are labeled by the doppleron causing them.

$n = 3$ peak in Fig. 2(c) is an unphysical artifact of our model due to neglect of spontaneous emission.

Dopplerons corresponding to three-photon resonance, $n = \pm 3$, were observed in the experiments of Stenlake et al. [8] by scanning the copropagating laser frequency ω_1. The minimum reflectivity of the $n = 3$ doppleron occurred for a laser detuning below the weak field value given by Eq. (14), consistent with $\Delta_L < 0$. The $n = 3$ doppleron corresponds to the absorption of two copropagating (ω_1) photons and stimulated emission of one counterpropagating (ω_2) photon; see Fig. 3 inset. Hence the shift in ω_1 for resonance will be half the light shift Δ_L. The $n = -3$ doppleron occurred at a laser detuning above the value given by Eq. (14). It corresponds to the absorption of two ω_2 photons and stimulated emission of one ω_1 photon; see Fig. 3 inset. Since one ω_1 photon is emitted, the expected shift of the $n = -3$ doppleron for resonance is the negative of the total light shift Δ_L.

Figure 3 shows the reflection probabilities obtained from our numerical model with the parameters of Table I. These parameters are within the experimental uncertainties of those reported by Stenlake et al. [8]. Hence Fig. 3 was obtained without adjustable parameters. It is the central result of this paper and should be compared to the experimental results presented in Fig. 2 of Stenlake et al. [8]. The reflection probabilities are plotted against the detuning Δ_1'' in the atom frame,

$$\Delta_1'' = \Delta_1 - v_x Q. \tag{16}$$

Reflection occurs when the detuning in the atom frame is positive. The $n = \pm 3$ dopplerons have nearly the frequencies found experimentally. The quantitative comparison of our results with the experiment is summarized in Table II. The $n = +3$ doppleron is within $2\pi \times 70$ MHz of the experimen-

TABLE II. Comparison of experimental and theoretical doppleron data. The frequency shift is that from the expected weak field resonance, Eq. (14). The data are frequencies in units of 2π GHz.

Parameter		Doppleron	Experiment	Model
Central frequency Δ_1''	$n = +3$	0.95	1.02
Frequency shift	$n = +3$	-0.18	-0.11
Width at half maximum	$n = +3$	0.24	0.15
Central frequency Δ_1''	$n = -3$	4.95	4.94
Frequency shift	$n = -3$	0.38	0.37
Width at half maximum	$n = -3$	>0.25	0.23

tal value. Most of this discrepancy can be accounted for by the difficulty in determining the central frequency of the experimental doppleron, Fig. 2 of [8], which is quite asymmetric. The calculated frequency of the $n = -3$ doppleron is well within the experimental error. The experimental width of the $n = +3$ doppleron is about 50% greater than the modeled value. This additional broadening is not unreasonable given the various nonideal aspects of the experiment, which are discussed at the end of this section. The experimental width of the $n = -3$ doppleron could not be determined with any accuracy but is certainly wider than the $n = +3$ doppleron, as required by our results.

Figure 3 also shows $n = \pm 5$ dopplerons, which were not observed in the experiment. They were presumably lost in the noise since they are shallower and narrower than the $n = \pm 3$ dopplerons. This can be understood as being due to the closer avoided crossings of the quasipotentials, and hence greater nonadiabatic transition rates, that occur for the $n = \pm 5$ case. Murphy et al. [13] reported fine scale structure of dopplerons due to resonances with quasibound states in the asymptotically forbidden quasipotential [12]. We have not attempted to resolve this structure, nor was it observed in the experiment. We did not attempt to find higher order dopplerons.

Both the experimental and numerical results show the $n = -3$ doppleron further shifted from the weak field resonance frequency than the $n = +3$ doppleron. An exact factor of 2 difference in the shifts is not seen due to the variation in the light shift with position, as previously discussed. This variation also contributes to the broadening of the doppleron resonances beyond that due to the natural atomic linewidth of $2\pi \times 10$ MHz.

The overall agreement is good considering the complexities and uncertainties of the experiment, and the idealizations of the numerical model. In particular the atoms are reflected from multiple Gaussian spots rather than the uniform fields that are assumed in the model. One effect of the nonuniform field distribution within the Gaussian spots is to reduce the effective reflection area as the detuning is increased [20]. The resulting decrease of the reflected atom signal with increasing detuning is apparent in Fig. 2 of Stenlake et al. [8].

The difference between the zero reflection predicted by the model at the $n = \pm 3$ dopplerons and the partial reflection observed in the experiment [8] is likely to be partly due to spontaneous emission. This regenerates ground level atoms, which may then be reflected instead of lost. Other factors expected to influence the agreement between the experiment
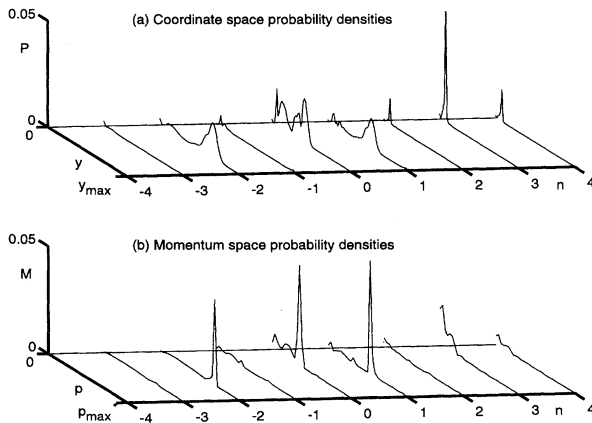
FIG. 4. Probability densities for a Ne atom undergoing diffraction. The time is $t = 2.6$ μs after the initial conditions given in Table I. (a) Coordinate-space probability densities $P = |\psi_n(y)|^2$ for $y \geq 0$. The surface is at $y = 0$ and $y_{max} = 3.74$ μm. (b) Momentum-space probability densities $M = |\psi_n(p_y)|^2$. $p_{max} \approx 170 \hbar k$. The parameters, given in Table I, are similar to those of Fig. 7 of Ref. [12], with an atomic beam angle of incidence of 50 mrad.

and the model include the angular divergence (< 0.5 mrad) and velocity spread (± 5 ms^{-1}) of the atomic beam, and possible incomplete overlap between the laser spots.

IV. DISCUSSION

Diffraction from evanescent-wave gratings has been predicted [11] and observed [9] with slowed atoms. In contrast our model does not predict diffraction of ground-state atoms in any parameter regime we have investigated for the fast atoms used by Stenlake et al. [8]. Indeed, diffraction was not observed in that experiment, despite the ability to adjust the relative velocity of the grating and atoms.

Murphy et al. [13] have also modeled the experiment of Stenlake et al. [8]. However, they considered only the retroreflected laser case, $\Delta_1 = \Delta_2$ and $E_1 = E_2$, and hence were not able to make quantitative comparisons with the experiment.

Our model shows diffraction of ground-state atoms for slowed neon beams, as predicted by Deutschmann et al. [12]; see Fig. 4. Figure 4(a) shows the coordinate-space

probability densities in the physical region $y > 0$. Figure 4(b) shows the momentum-space probability densities for $p_y > 0$. A comparison of the wave functions in Figs. 4(a) and 4(b) indicates that the wave packets in Fig. 4(a) have a positive y velocity and hence are moving away from the interface. The mean momentum $\langle p_y \rangle$ of the $n = -2$ wave function is greater than that of the $n = 0$ wave function. Hence it corresponds to high angle diffraction. The total outgoing probability is about 25%, with that in the $n = -2$ wave function about 6%. The wave functions with $n = 1$ and $n = 3$ correspond to excited atomic states and hence would not be observed experimentally due to spontaneous emission, as previously discussed.

Figure 4 was obtained with a time step of $\Delta t = 0.1$ ns, a y grid of 4096 points with a lattice spacing of 1.83 nm, and using ψ_n for $n \in (-11, \ldots, 11)$, although only $n \in (-4, \ldots, 4)$ are shown. The result is consistent with the predictions of Deutschmann et al. [12] based on the quasi-potential method.

Christ et al. [9] observed diffraction with slow metastable neon. We have modeled the conditions of that experiment (not shown) and found no significant atomic diffraction. This suggests that the physics of the diffraction that is seen in this experiment is not encompassed by the two-level model. This is perhaps not surprising since multiple levels enrich the physics and provide new diffraction channels [21]. The different coupling strengths of the transitions to the light produce different light shifts and hence an increased range of kinetic energies that the atoms may gain from the field.

Our model could be improved by including the multistate hyperfine structure of real atoms. Spontaneous emission could also be included using a stochastic wave-function method [22,23]. However, such improvements would substantially increase the computational time. Including the Gaussian laser spot shape is also possible but probably not practical with our type of model. In summary, we have shown that a numerical solution of the two-level Schrödinger equation, without adjustable parameters, agrees quantitatively with the experimental observations of dopplerons in evanescent light fields by Stenlake et al. [8].

ACKNOWLEDGMENTS

[1] V.I. Balykin, V.S. Letokhov, Yu.B. Ovchinnikov, and A.I. Sidorov, Phys. Rev. Lett. 60, 2137 (1988).

[2] J.V. Hajnal, K.G.H. Baldwin, P.T.H. Fisk, H.-A. Bachor, and G.I. Opat, Opt. Commun. 73, 331 (1989).

[3] M.A. Kasevich, D.S. Weiss, and S. Chu, Opt. Lett. 15, 607 (1990).

[4] C.G. Aminoff, A.M. Steane, P. Bouyer, P. Desbiolles, J. Dalibard, and C. Cohen-Tannoudji, Phys. Rev. Lett. 71, 3083 (1993).

[5] W. Seifert, C.S. Adams, V.I. Balykin, C. Heine, Yu. Ovchinni-

kov, and J. Mlynek, Phys. Rev. A 49, 3814 (1994).

[6] W. Seifert, R. Kaiser, A. Aspect, and J. Mlynek, Opt. Commun. 111, 566 (1994).

[7] S. Feron, J. Reinhardt, M. Ducloy, O. Gorceix, S. Nic Chormaic, Ch. Miniatura, J. Robert, J. Baudon, V. Lorent, and H. Haberland, Phys. Rev. A 49, 4733 (1994).

[8] B. W. Stenlake, I.C.M. Littler, H.-A. Bachor, K.G.H. Baldwin, and P.T.H. Fisk, Phys. Rev. A 49, 16 (1994).

[9] M. Christ, A. Scholz, M. Schiffer, R. Deutschmann, and W. Ertmer, Opt. Commun. 107, 211 (1994).

[10] R.J. Cook and R.K. Hill, Opt. Commun. **43**, 258 (1982).

[11] J.V. Hajnal and G.I. Opat, Opt. Commun. **71**, 119 (1989).

[12] R. Deutschmann, W. Ertmer, and H. Wallis, Phys. Rev. A **47**, 2169 (1993).

[13] J.E. Murphy, L. Hollenberg , and A.E. Smith, Phys. Rev. A **49**, 3100 (1994).

[14] Sze M. Tan and D.F. Walls, Phys. Rev. A **50**, 1561 (1994).

[15] U. Janicke and M. Wilkens, Phys. Rev. A **50**, 3265 (1994).

[16] E. Kyrölä and S. Stenholm, Opt. Commun. **22**, 123 (1977).

[17] C. S. Adams, M. Sigel, and J. Mlynek, Phys. Rep. **240**, 1 (1994).

[18] P. Marte, R. Dum, R. Taieb, and P. Zoller, Phys. Rev. A **47**, 1378 (1993).

[19] R. Kosloff, J. Phys. Chem. **92**, 2087 (1988).

[20] N. Snoad, Honours year thesis, Australian National University, 1993 (unpublished).

[21] R. Deutschmann (private communication).

[22] H. J.Carmichael, *An Open Systems Approach to Quantum Optics*, Lecture Notes in Physics Vol. 18 (Springer-Verlag, Berlin, 1993).

[23] K. Molmer, Y. Castin, and J. Dalibard, J. Opt. Soc. Am. B **10**, 524 (1993).